PRL 108, 076801 (2012) PHYSICAL REVIEW LETTERS week ending 17 FEBRUARY 2012

Spectroscopy of Single Donors at ZnO(0001) Surfaces

Hao Zheng,[1,*] Jörg Kröger,[2] and Richard Berndt[1]
[1]Institut für Experimentelle und Angewandte Physik, Christian-Albrechts-Universität zu Kiel, D-24098 Kiel, Germany
[2]Institut für Physik, Technische Universität Ilmenau, D-98693 Ilmenau, Germany

(Received 16 September 2011; published 13 February 2012)

Donors near the polar (0001) surface of nominally undoped ZnO were investigated with scanning tunneling microscopy at 5 K. Spatially resolved spectroscopy reveals single and double charging. Equidistant peaks in spectra of ionized donors are attributed to polaron excitation. The data are consistent with doping due to Zn interstitials or complexes.

DOI: 10.1103/PhysRevLett.108.076801 PACS numbers: 73.20.Hb, 68.37.Ef, 73.20.Mf

ZnO has been widely investigated as a material for piezo-, micro-, and optoelectronic devices [1,2]. Although the band gap of ZnO in the wurtzite structure is as large as 3.4 eV, undoped material exhibits n-type conductivity at room temperature. The residual conductance can lead to self-compensation, which impedes p-type doping [3]. The conductivity has been attributed to native defects such as interstitial Zn [4], Zn with O vacancies [5], or Zn with substitutional N [6], as well as to H impurities [7,8]. Despite its importance for applications the origin of the residual conductance is still a subject of much controversy [1,9]. A similar problem exists for a wide class of related materials, transparent conductive oxides. Partially this unsatisfactory situation may be caused by the materials used. Depending on the growth method, the conductivity may be due to different donors [10].

Scanning tunneling microscopy (STM) has been shown to be sensitive to subsurface dopants in GaAs [11] and to the charge state of defects [12–14]. Here this method is employed to investigate the ionization of donors in the wide-gap material ZnO. Double charging and vibronic features are observed in scanning tunneling spectra, which are consistent with intrinsic Zn defects and are difficult to reconcile with H doping.

The experiments were performed in a homebuilt ultrahigh vacuum STM operated at 5 K. Commercial wurtzite ZnO(0001) single crystals (MaTeck GmbH, Germany) were cleaned by cycles of Ar^+ bombardment (ion energy $1, \ldots, 2$ keV) and subsequent annealing at $\approx 700\,^\circ\mathrm{C}$ for 1 h [15]. The nominally undoped material had been produced by hydrothermal growth, and shows light yellow color. After their preparation samples were transferred *in vacuo* to the STM chamber with a residual gas pressure below 2×10^{-9} Pa. Au tips were cut from polycrystalline wire and cleaned by Ar^+ bombardment and annealing prior to mounting to the STM. Constant-current STM images were recorded with the bias voltage applied to the sample. Spectra and maps of the differential conductance (dI/dV) were acquired using a lock-in amplifier with 30 $\mathrm{mV_{rms}}$ modulation of the bias.

The polar ZnO(0001) surface is perpendicular to the bulk electrostatic dipole moment and, therefore, is not atomically flat [16]. The low temperature STM image in Fig. 1(a) shows the typical morphology of the clean surface. It is similar to previously reported results from room temperature measurements [16]. Like in the case of

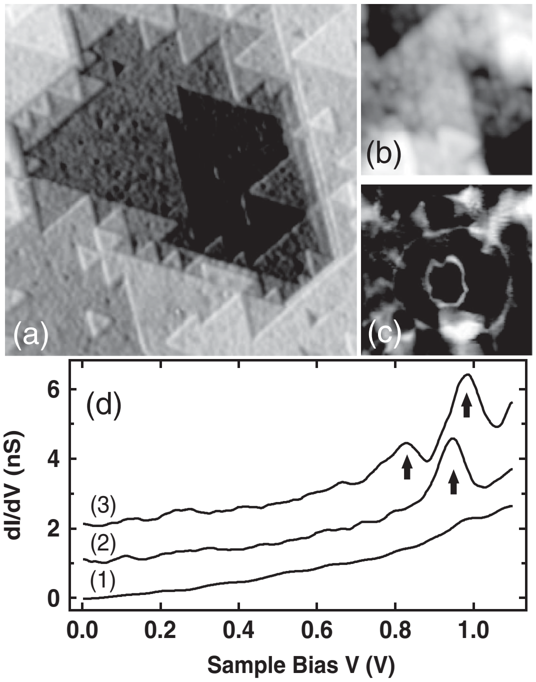

FIG. 1. (a) Constant-current STM image of clean ZnO(0001) at 5 K (50×50 nm^2, 2 V, 100 pA). To enhance the visibility of small features such as atomic steps, the image displays a superposition of the apparent height z and its derivative dz/dx. The image covers a height range of 7 ZnO layers. (b) STM image of an area containing a donor (15×15 nm^2, 1 V, 1 nA). (c) Map of the differential conductance (dI/dV) measured simultaneously with (b). (d) dI/dV spectra measured (1) outside of two rings, (2) between the outer and the inner ring, and (3) inside of the rings. The curves are vertically offset for clarity. Arrows indicate peaks due to ionization of the donor. Tunneling parameters prior to disabling feedback were 1.1 V, 1 nA.

wurtzite GaN [17,18], large terraces with jagged step edges and triangular islands and vacancies indicate that the wurtzite structure of the sample is intact and no phase transition has occurred during the cooling process. Even at a sample temperature of 5 K, images of the surface can be acquired at rather low bias voltages down to 0.6 V, which indicates a high electron density of the material. Figures 1(b) and 1(c) display a STM image and a simultaneously recorded dI/dV map of a smaller surface area. The STM image shows the typical terrace structure with two triangular islands close to the bottom. In the dI/dV map, irregular variations are observed, which exhibit some correlation with the terrace structure. However, the predominant features are two concentric rings with diameters of ≈ 3 nm and ≈ 10 nm. dI/dV spectra measured at the interior of the two rings [Fig. 1(d)] reveal two peaks at ≈ 0.82 and ≈ 0.98 V. The lower peak moves to ≈ 0.94 V and the higher peak disappears from the spectra in the annulus between the rings. Both peaks are absent outside the rings.

We suggest that a buried donor which is capable of donating two electrons and tip-induced band bending causes the features in dI/dV spectra and maps. Figure 2 shows schematic energy diagrams of a ZnO-Au tunneling junction at various voltages. The surface state of ZnO(0001) is not considered as it is located well outside the band gap [19]. At zero bias [Fig. 2(a)] the work function difference of the tip and the sample bends the band upwards. The local band bending depends on the distance from the surface. U denotes the band bending at the position of a near-surface donor. The defect level D^0 is located below the Fermi energy of the sample $E_F^{(S)}$ by an energy Δ. At positive sample voltage V, current flows to the conduction band of ZnO. The low carrier density in the oxide does not fully screen the electrical field in the semiconductor and the band bending at the donor is increased in proportion to the bias by an amount βV. β is the ratio of the voltage drop between the ZnO bulk and the donor to the applied bias. As a result of the field penetration, the defect level is shifted closer to $E_F^{(S)}$. At bias $V_1 = \Delta/\beta$, D^0 aligns with $E_F^{(S)}$ and a first ionization of the donor takes place [Fig. 2(b)] [20]. The charge of the donor affects the local potential [Fig. 1(c)], thus inducing a rapid rise of the current and a corresponding first peak of the dI/dV spectrum at ≈ 0.82 V. Upon further increase of the bias, the level D^+ of the charged donor reaches $E_F^{(S)}$ and a second ionization takes place [≈ 0.98 V in Fig. 1(d)].

The above model is also consistent with the lateral variation of the spectra and the features in dI/dV maps. In these maps (Fig. 3) the two concentric, nearly circular rings are observed to shrink as the voltage decreases. While the inner ring fades away between 1 and 0.9 V, the remaining ring collapses to a bright spot at 0.6 V. The penetration of the electrical field into the sample is strongest directly under the tip apex and decreases as one moves away in a lateral direction. As a result, the conditions for a conductance peak to occur, $E_F^{(S)} = D^0$ and $E_F^{(S)} = D^+$, are fulfilled at certain lateral distances of the tip from the donor, namely, the radii of the outer and inner ring, respectively. At low bias, ionization is only possible when the tip apex is directly above the donor [Fig. 3(j)]. A more detailed three-dimensional analysis of tip-induced band bending, which would possibly reveal the ionization threshold of the dopant, is difficult and requires, e.g., information on the tip

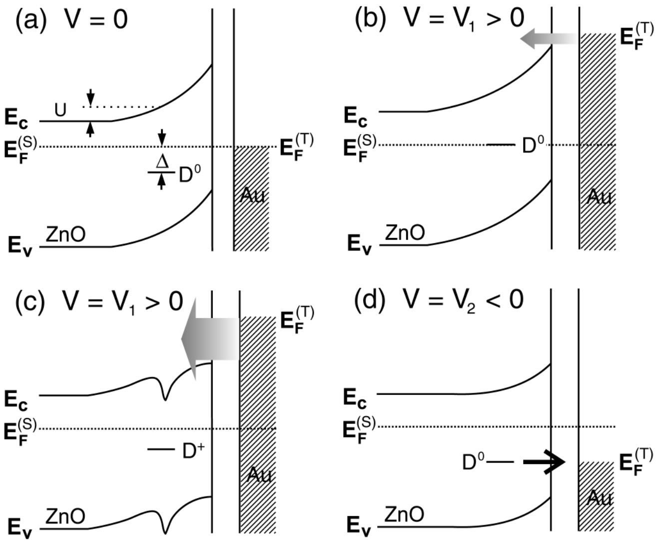

FIG. 2. Schematic energy diagrams (not to scale) of a ZnO/Au tunneling junction. E_C and E_V indicate the conduction band minimum and valence band maximum of ZnO. $E_F^{(S)}$ and $E_F^{(T)}$ are the Fermi levels of ZnO and the Au tip. D^0 and D^+ are defect levels of a neutral and a singly charged donor, respectively. The band bending depends on the distance to the surface. The local band bending at the position of the donor is denoted as U. (a) Zero bias. (b) Positive bias with current from the Au tip to the ZnO conduction band indicated by a shaded arrow. At the chosen bias $V = V_1$, single ionization of the donor occurs. (c) Upon ionization, the local band bending at the donor is modified and the current is increased. (d) Negative bias. At $V = V_2$ single ionization of the donor occurs by tunneling from the donor level to the tip (black arrow).

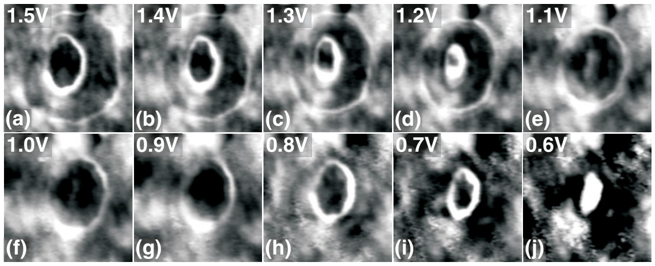

FIG. 3 (color online). Constant-current dI/dV maps acquired at the indicated voltages of a surface area containing a donor (12×12 nm^2, 1 nA).

shape, the depth of the donor, and the band structure of the oxide.

Single ringlike structures were previously found around Si donors in GaAs [14]. Single rings were also observed from C_{60} films doped with alkali metal atoms [13]. Depending on the molecule-atom interaction, the ring diameters increased or decreased with increasing voltage. Double rings have not previously been reported. Buried dopants in InAs may also induce Friedel oscillations of the charge density, which may lead to multiple-ring structures in dI/dV maps [21]. However, the sharpness of the rings on ZnO as observed in the present experiments are inconsistent with Friedel oscillations.

In 250 nm^2 areas we observed between 9 and 19 donors. For a donor that can be doubly charged, the sheet carrier concentration is estimated to $\approx 0.7, \ldots, 1.5 \times 10^{12}\ \mathrm{cm}^{-2}$. This concentration is consistent with previous Hall effect data from hydrothermally grown ZnO crystals [22].

Having located donors in dI/dV maps we now focus on their spectra at negative sample voltage, which display a series of equidistant peaks (Fig. 4, solid lines). Spectra recorded elsewhere are featureless (Fig. 4, dashed line). In particular, the clear donor-related peaks (Fig. 4, middle curve) vanish when the tip is moved in a lateral direction by less than 1.5 nm. This drastic dependence on the tip position, which is different from the positive-bias case, suggests a direct involvement of donor states in the tunneling process. We attribute the equidistant peaks to the excitation of longitudinal optical (LO) phonons of ZnO(0001) via resonant tunneling through the donor level closest to the substrate Fermi energy.

At negative bias the local band bending shifts D^0 away from $E_F^{(S)}$, which prevents the ionization of the donor. However, when D^0 is aligned with the Fermi level of the tip at a bias V_2 [Fig. 2(d)], an electron from the donor level may transfer to the tip. This occurs at $|V_2| = \beta|V_2| + \Delta$. The donor level will be refilled from bulk or defect states of the ZnO crystal. The charge state of the donor affects the local atomic lattice of ZnO. Therefore, tunneling from the donor to the tip efficiently couples to the excitation of LO phonons.

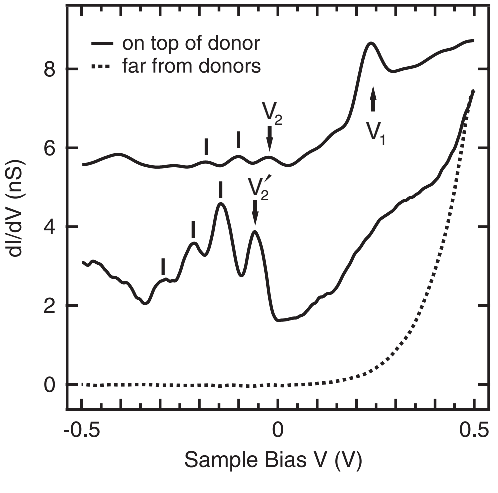

FIG. 4. dI/dV spectra measured above two different donors (solid lines) and far from any donors (dashed line). The curves are vertically offset for clarity. Bars indicate peaks attributed to polaron excitation. Arrows point to the ionization peaks at positive (V_1) and negative (V_2) voltages. Tunneling parameters prior to disabling feedback were 0.5 V and 1 nA.

In analyzing the vibrational progression, the voltage drop in the semiconductor has to be considered. Following Ref. [23] we estimate β from the equations above as $\beta = |V_2|/(V_1 + |V_2|)$. From Fig. 4 (upper curve), $V_1 \approx 235$ meV and $V_2 \approx -25$ meV, we obtain $\beta \approx 10\%$. These values depend on the depth of the subsurface donor as illustrated by the middle curve in Fig. 4. There the onset of the polaron excitation occurs at more negative bias and the ionization peak at positive bias is shifted out of range, which is indicative of a donor at larger depth. After correction of the peak distances with β, we obtain a spacing of (71 ± 5) mV from different donors. This spacing matches the energies of the polar A_1 and E_1 LO phonons (72 and 73 meV) [24,25]. The value from the dI/dV spectra of Fig. 4 is slightly different from these energies. This difference between the (bare) phonon energy $\hbar\omega$ and the observed line spacing $\alpha\hbar\omega$ can be rationalized in terms of the Fröhlich constant α, which takes into account the polaron character of the excitation. From our value and Raman data [24], we find $\alpha = 0.99 \pm 0.06$, which is close to calculated values, $\alpha = 1.0$ [26] or $= 1.19$ [27]. Similar coupling between vacancy sites or adatoms and LO phonons has been observed for NaCl films [28] and for Si(111) [29].

The experimental results presented above can be used to discriminate between various suggested donors. H interstitials ($\mathrm{H_I}$) were proposed as the source of the residual conductance of ZnO [7]. The energy of the local vibrational mode of $\mathrm{H_I}$, ≈ 412 meV (3326.3 cm^{-1}) [30], which has been attributed to an O-H stretching mode, is far away from the vibrational energy observed here. Moreover, high concentrations of $\mathrm{H_I}$ were reported to reduce the Raman intensity of the LO phonon [31]. Recently it was shown that H trapped in an O vacancy ($\mathrm{H_O}$) may also act as a shallow donor [8]. However, according to calculations both $\mathrm{H_I}$ and $\mathrm{H_O}$ donate a single electron only [7,8]. Furthermore, high temperature annealing of ZnO reduces or even removes the H-related shallow donor state [31,32]. A similar effect may be expected for H_2 in ZnO. Moreover, H_2 molecules at interstitial sites were found to be neutral, and thus are not a likely source of residual conductance [33,34]. On the contrary, annealing increases the density of native defects, $\mathrm{Zn_I}$ and oxygen vacancies ($\mathrm{V_O}$), and enhances the Raman intensity of the LO phonon [35,36]. Both $\mathrm{Zn_I}$ and $\mathrm{V_O}$ can be doubly charged [9,37] as observed from the donors in the present samples. While the ionization energy of $\mathrm{Zn_I}$ is only 30 meV [4], $\mathrm{V_O}$ has been shown to induce a deep level with an ionization energy of 2.1 eV [38]. The sample voltages used here, e.g., $V < 1.1$ V in Fig. 1(d), are too small to make this ionization possible through single-electron processes. Photoexcitation of $\mathrm{V_O}$ to a metastable shallow donor state [39] is very unlikely in our experiment, where the sample was kept in the dark for weeks and no time-dependent changes were observed. Moreover, calculations [39] find the metastable shallow donor above E_C, which appears to be inconsistent with our observations of double charging. Therefore, Zn interstitials remain as a suitable candidate for explaining the conductivity of our samples. Recent work has suggested that defect complexes rather than isolated defects may be at the origin of shallow levels. While the high formation energy of $\mathrm{Zn_I}$ appears to exclude these interstitials, $\mathrm{Zn_I}$-$\mathrm{V_O}$ and $\mathrm{Zn_I}$-$\mathrm{N_O}$ (N substituting O) complexes form more readily [5,6,35]. Summarizing the discussion, our experimental data from *in vacuo* annealed ZnO(0001) surfaces are difficult to reconcile with H or $\mathrm{V_O}$, but are consistent with $\mathrm{Zn_I}$ or a related complex.

In summary, ZnO(0001) samples were prepared by Ar bombardment and annealing to ≈ 700 °C. Scanning tunneling spectroscopy of donors in ZnO(0001) reveals single and double charging as well as local excitation of polarons. The data indicate that the donors are Zn interstitials or complexes.

Financial support by the Deutsche Forschungsgemeinschaft through SFB 855 and discussions with Ph. Ebert, M. Grundmann, E. Pehlke, M. Rohlfing, E. Runge, S. Shokhovets, and M. Wenderoth are gratefully acknowledged.

---

*zheng@physik.uni-kiel.de

[1] Ü. Özgür, Ya. I. Alivov, C. Liu, A. Teke, M. A. Reshchikov, S. Dogan, V. Avrutin, S.-J. Cho, and H. Morkoç, J. Appl. Phys. **98**, 041301 (2005).

[2] H. Zheng, Z. X. Mei, Z. Q. Zeng, Y. Z. Liu, L. W. Guo, J. F. Jia, Q. K. Xue, Z. Zhang, and X. L. Du, Thin Solid Films **520**, 445 (2011).

[3] K. G. Saw, K. Ibrahim, Y. T. Lim, and M. K. Chai, Thin Solid Films **515**, 2879 (2007).

[4] D. C. Look, J. W. Hemsky, and J. R. Sizelove, Phys. Rev. Lett. **82**, 2552 (1999).

[5] Y.-S. Kim and C. H. Park, Phys. Rev. Lett. **102**, 086403 (2009).

[6] D. C. Look, G. C. Farlow, P. Reunchan, S. Limpijumnong, S. B. Zhang, and K. Nordlund, Phys. Rev. Lett. **95**, 225502 (2005).

[7] Ch. G. Van de Walle, Phys. Rev. Lett. **85**, 1012 (2000).

[8] A. Janotti and Ch. G. Van de Walle, Nature Mater. **6**, 44 (2006).

[9] F. Oba, M. Choi, A. Togo, and I Tanaka, Sci. Tech. Adv. Mater. **12**, 034302 (2011).

[10] P. D. C. King and T. D. Veal, J. Phys. Condens. Matter **23**, 334214 (2011).

[11] J. F. Zheng, X. Liu, N. Newman, E. R. Weber, D. F. Ogletree, and M. Salmeron, Phys. Rev. Lett. **72**, 1490 (1994).

[12] Ph. Ebert, G. Cox, U. Poppe, and K. Urban, Ultramicroscopy **42–44**, 871 (1992).

[13] N. A. Pradhan, N. Liu, C. Silien, and W. Ho, Phys. Rev. Lett. **94**, 076801 (2005).

[14] K. Teichmann, M. Wenderoth, S. Loth, R. G. Ulbrich, J. K. Garleff, A. P. Wijnheijmer, and P. M. Koenraad, Phys. Rev. Lett. **101**, 076103 (2008).

[15] Lacking information on the emissivity of our ZnO crystals, the sample temperature was estimated using an infrared pyrometer, which was focused on the Mo sample holder.

[16] O. Dulub, U. Diebold, and G. Kresse, Phys. Rev. Lett. **90**, 016102 (2003).

[17] M. H. Xie, S. M. Seutter, W. K. Zhu, L. X. Zheng, H. S. Wu, and S. Y. Tong, Phys. Rev. Lett. **82**, 2749 (1999).

[18] H. Zheng, M. H. Xie, H. S. Wu, and Q. K. Xue, Phys. Rev. B **77**, 045303 (2008).

[19] R. T. Girard, O. Tjernberg, G. Chiaia, S. Soderholm, U. O. Karlsson, C. Wigren, H. Nylen, and I. Lindau, Surf. Sci. **373**, 409 (1997).

[20] To validate the energy diagrams of Fig. 2, we use the upper data set in Fig. 4, where $\beta = 0.1$. The local band bending U at $V = 0$ may be estimated from the work function of the Au tip, $\Phi = 5.1$ eV, and the electron affinity of ZnO, $\chi = 4.1$ eV, as $U = \beta(\Phi - \chi) \approx 100$ meV. As the donor is close to but not in the surface layer, the band bending right at the surface may be slightly larger. However, tunneling to subsurface layers may occur for sample voltages $V > 100$ mV, which is lower than the ionization peak $V_1 = 235$ mV. Together these values show that the Fermi level of the tip is located above the conduction band edge when the D^0 is aligned with the Fermi level of the sample. This corresponds to the schematic energy diagrams shown in Fig. 2.

[21] K. Kanisawa, M. J. Butcher, H. Yamaguchi, and Y. Hirayama, Phys. Rev. Lett. **86**, 3384 (2001).

[22] D. C. Look, Surf. Sci. **601**, 5315 (2007).

[23] S. W. Wu, G. V. Nazin, X. Chen, X. H. Qiu, and W. Ho, Phys. Rev. Lett. **93**, 236802 (2004).

[24] N. Ashkenov, B. N. Mbenkum, C. Bundesmann, V. Riede, M. Lorenz, D. Spemann, E. M. Kaidashev, A. Kasic, M. Schubert, M. Grundmann, G. Wagner, H. Neumann, V. Darakchieva, H. Arwin, and B. Monemar, J. Appl. Phys. **93**, 126 (2003).

[25] The polarizations of the A_1 and E_1 modes are perpendicular and parallel, respectively, to the (0001) surface plane. Presumably the A_1 LO phonon is preferably excited by the tunneling current.

[26] W. S. Baer, Phys. Rev. **154**, 785 (1967).

[27] Y. Imanaka, M. Oshikiri, K. Takehana, T. Takamasu, and G. Kido, Physica (Amsterdam) **298B**, 211 (2001).

[28] J. Repp, G. Meyer, S. Paavilainen, F. E. Olsson, and M. Persson, Phys. Rev. Lett. **95**, 225503 (2005).

[29] M. Berthe, A. Urbieta, L. Perdigao, B. Grandidier, D. Deresmes, C. Delerue, D. Stievenard, R. Rurali, N. Lorente, L. Magaud, and P. Ordejon, Phys. Rev. Lett. **97**, 206801 (2006).

[30] M. D. McCluskey, S. J. Jokela, K. K. Zhuravlev, P. J. Simpson, and K. G. Lynn, Appl. Phys. Lett. **81**, 3807 (2002).
[31] E. V. Lavrov, F. Herklotz, and J. Weber, Phys. Rev. B **79**, 165210 (2009).
[32] G. A. Shi, M. Saboktakin, M. Stavola, and S. J. Pearton, Appl. Phys. Lett. **85**, 5601 (2004).
[33] S. Zh. Karazhanov and A. G. Ulyashin, Phys. Rev. B **78**, 085213 (2008).
[34] M.-H. Du and K. Biswas, Phys. Rev. Lett. **106**, 115502 (2011).
[35] J. Sann, J. Stehr, A. Hofstaetter, D. M. Hofmann, A. Neumann, M. Lerch, U. Haboeck, A. Hoffmann, and C. Thomsen, Phys. Rev. B **76**, 195203 (2007).
[36] X. Q. Wei, B. Y. Man, M. Liu, C. S. Xue, H. Z. Zhuang, and C. Yang, Physica (Amsterdam) **388B**, 145 (2007).
[37] A. Janotti and Ch. G. Van de Walle, Phys. Rev. B **76**, 165202 (2007).
[38] S. M. Evans, N. C. Giles, L. E. Halliburton, and L. A. Kappers, J. Appl. Phys. **103**, 043710 (2008).
[39] S. Lany and A. Zunger, Phys. Rev. B **72**, 035215 (2005).